N70 33228

NASA TECHNICAL TRANSLATION

NASA TT F-12, 968

THE STRUCTURE OF LOW-DENSITY SUPERSONIC JETS

V. I. Nemchenko, N. I. Yushchenkova

Translation of "Struktura sverkhzvukovoy strui nizkoy plotnosti," Zhurnal Prikladnoy Mekhaniki i Tekhnicheskoy Fiziki, No. 6, 1969
pp. 110 - 115

CASE FILE COPY

NATIONAL AERONAUTICS AND SPACE ADMINISTRATION
WASHINGTON, D.C. 20546 JUNE 1970

THE STRUCTURE OF LOW-DENSITY SUPERSONIC JETS

V. I. Nemchenko, N. I. Yushchenkova (Moscow)

ABSTRACT. The results of an experimental investigation conducted in a low-density wind tunnel, to determine the structure of a supersonic jet for different discharge conditions are given. Procedures used to obtain the results are described, and the effect of the Mach number, and of flow rarefaction, on the formation of the flow in the normal shock wave region are discussed.

The use of supersonic jets to obtain intensive molecular beams and /110* high velocity flows of low temperature plasma has stimulated the development of experimental and theoretical work on the structure of underexpanded supersonic jets. The structure of the initial section of a supersonic underexpanded jet can be characterized by the position, dimensions, and shape of the breakdown shock.

Theoretical assessments, and some experimental data concerning the shape of the pendulous shock and the position and diameter of the normal shock, are cited in references [1-7]. However, the majority of the investigations are for the conditions that pertain for a perfect gas flow in the continuum mode.

Changes in the structure of the flow should be expected with a reduction in the density of the jet because the transfer processes, the role of which increases with rarefaction, have a significant effect on the formation of the pendulous shock, and on the jet boundary.

This paper contains the results of an experimental investigation of the structure of a supersonic jet of air for different discharge conditions $10 \leq n \leq 10^4$ $1.15 \leq M_a \leq 3.3$, $10^{-4} \leq K_* = \lambda_*/d_* \leq 10^{-3}$, where M_a is the Mach number in the nozzle section, λ_* is the length of the free run of the molecule in the critical throat section of the nozzle, d_* is

---

* Numbers in the margin indicate pagination in the foreign text.

the diameter of the critical throat section of the nozzle, n is the ratio of the pressure in the nozzle section to the pressure in surrounding space, and these results explain the effect of high ratios of pressures n, Mach numbers M_a, and the rarefaction of the flow on the structure of a supersonic, underexpanded jet. The Knudsen number, K_*, and the parameter $C = K_*\sqrt{n}$, are used for the characteristics of flow rarefaction.

1. The experiment was conducted in the low density wind tunnel described in [8]. Air, heated to ~600°K to prevent condensation during adiabatic expansion [9], was used as the working gas. The gas jet discharged through a supersonic conical nozzle into a chamber at reduced pressure. Nozzle dimensions, and jet discharge conditions, are listed in Table 1, where the upper row in column d is the nozzle diameter in the critical throat section, and the lower row is the diameter of the nozzle section, ξ_o is the nozzle semidivergence angle; the upper row in the M column lists the values of the Mach number in the nozzle section, M_a', computed for isentropic gas expansion, and the lower row lists the Mach number in the nozzle section obtained by measuring the total head pressure, p_o'; p_o is the pressure in an adiabatically decelerated flow, in mm mercury column.

The following parameters were measured during the experiment: pressure p_o and temperature T_o in the adiabatically decelerated flow; p_o', the total head pressure; and p_1, the vacuum chamber pressure. A 0.8 mm diameter pitot tube was used to measure the total head pressure. Viscosity corrections were introduced using the methodology described in [8]. The results of the p_o and T_o measurements were used to compute the parameters of the flow in the critical throat section of the nozzle, while those of the p_o' and p_o measurements were used to compute the parameters in the nozzle section and in the jet.

Pressures in the range from 10^{-3} to 10^{-1} mm mercury column were measured by an LT-2 thermocouple manometer calibrated against a compression manometer for higher pressures, while those from 10^{-2} to 10 mm mercury column were measured by a VR-3 radioactive manometer, which too was calibrated against a compression manometer. Pressure in the range from 1 to

700 mm mercury column was measured with U-shaped oil and mercury manometers. The relative error in measuring the pressures in the range from 10^{-3} to 1 mm mercury column was within 3%, while that in the range from 1 to 700 mm mercury column was within 1%.

Table 1 /111

d	ξ_0	M	p_0	K_*	n
1	55′	1.14	700	$2.14\cdot10^{-4}$	100—8000
1.01			500	$3.01\cdot10^{-4}$	
			300	$5.01\cdot10^{-4}$	
1.85	6°12′	2.5	700	$1.16\cdot10^{-4}$	17—785
3		2.23—2.27	500	$1.62\cdot10^{-4}$	
			300	$2.7\cdot10^{-4}$	
			150	$5.4\cdot10^{-4}$	
			50	$1.62\cdot10^{-4}$	
1.85	7°57′	2.75	700	$1.16\cdot10^{-4}$	37—1000
3.35		2.5	500	$1.62\cdot10^{-4}$	
			300	$2.7\cdot10^{-4}$	
			150	$5.4\cdot10^{-4}$	
1.85	10°05′	3	700	$1.16\cdot10^{-4}$	20—500
3.83		2,8	500	$1.62\cdot10^{-4}$	
			300	$2.7\cdot10^{-4}$	
1.5	10°20′	3.5	700	$1.43\cdot10^{-4}$	24—227
4.4		3.4	500	$2.1\cdot10^{-4}$	
			300	$3.34\cdot10^{-4}$	

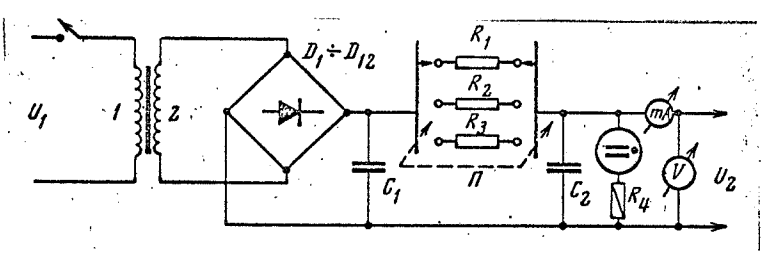

Figure 1. Schematic diagram of the supply to the discharge gap

The glow discharge flow visualization technique, widely used to investigate the flow of a supersonic gas over bodies, was used to investigate the structure of the initial section of the supersonic, underexpanded jet in the case of low flow densities when the Topler technique could not be

used. For example, the investigations of the flow of a hypersonic rarified gas over a plate with a sharp leading edge conducted in [10] using the glow discharge technique, the schlieren technique, film sensors, hot-wire anemometers, and pitot tubes revealed that the shapes of the shock waves obtained by the different methods coincided.

The anode for the discharge gap used to visualize the field of a jet stream was a quartz reinforced molybdenum rod, and the cathode was a thermostatically regulated nozzle. Figure 1 is the diagram of the supply for the discharge gap. D_1, ..., D_{12} are the rectifier bridge diodes. U_1 and U_2 are the voltages across the rectifier input and output, respectively. An autotransformer was used to vary voltage U_1 from 10 to 250 volts. The discharge gap current, I, and the voltage drop, V, across the gap were selected experimentally in the range $0.5 \leq I \leq 40$ ma, $300 \leq V \leq 700$ volt for concrete flow conditions. The power consumed by the discharge gap was 20 watts, maximum. /112

The measurements made of the distribution of the total head pressure along the axis of the jet during discharge, and without discharge, showed that the discharge had no effect on the flow of gas when $I < 40$ ma. The concentrations of free electrons in the jet, based on data obtained with a Langmuir probe, were not in excess of 10^8 to 10^9 cm^{-3}, corresponding to a gas ionization of 10^{-6}. When the degree of ionization is below 10^{-3} to 10^{-4}, the effect of the discharge on the field of the gas dynamic parameters in the jet can be ignored [11], so the glow discharge flow visualization technique can be used to investigate the geometry and the positions of shock waves that result during the discharge of a supersonic underexpanded jet.

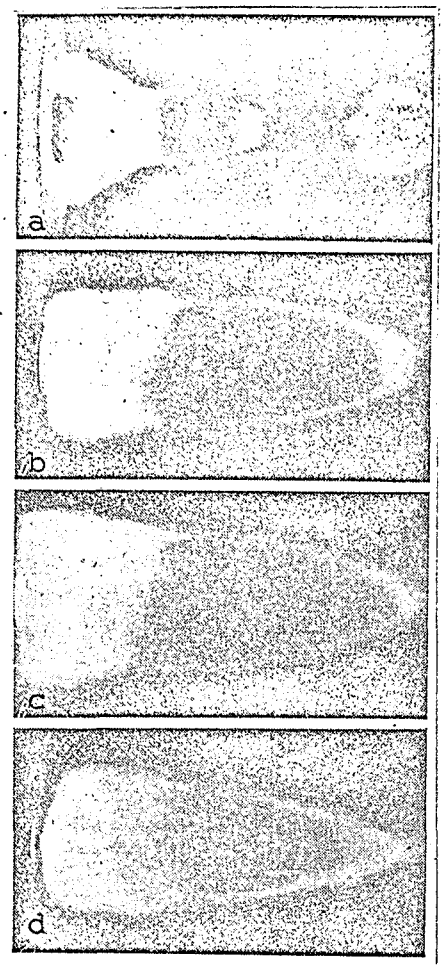

Figure 2. Results of visualization of a jet in a glow discharge. The values n = 56, 176, and 185 correspond to the case of $M_a = 2.8K_* \approx 1.62 \times 10^{-4}$, (a), (b), (c), and n = 87 corresponds to the case of $M_a \approx 3.3\ K_* \approx 1.43 \times 10^{-4}$, (d).

2. The jet photography obtained (see fig. 2a, b, c, d, for example) established the geometry of the breakdown shock wave in a supersonic underexpanded jet of air under different discharge conditions; x_o is the distance to the breakdown shock wave along the jet axis, D is the maximum diameter of the pendulous shock wave, D_o is the diameter of the normal shock wave, α is the angle at the triple point between the incident shock wave and the direction of the axis. Results of the investigation show that at high flow densities $K_*\sqrt{n} < 10^{-3}$ and γ = constant when the

rarefaction effect is insignificant, the ratios D/x_o, D_o/x_o (Table 2) will be functions of the Mach number in the nozzle section and do not depend on n, which characterizes the self-similarity feature of the jet structure. A similar result was obtained in [1] for a jet with $M_a \approx 1$ using the Toplar technique.

The position of the normal shock wave can be determined by the linear function $\sqrt{n}$

$$x_o/r_a = A\sqrt{n} \tag{2.1}$$

where

r_a is the radius of the nozzle exit section;

A is the proportionality factor, determined by the empirical dependency

$$A \approx 1.38 \sqrt{\gamma} M_a \tag{2.2}$$

proposed in [4].

In the formula at (2.2), γ is the ratio of the specific heats. The values of the A coefficients (points 2 in Fig. 3a), obtained by processing the jet photography, visualized in a glow-discharge, agree well with the dependency at (2.2) and with the results of the experiments performed by other authors [1,2] obtained by the schlieren method in the case of high flow densities (points 3 and 4 in Fig. 3a) right up to some limit Mach number, M_{al}.

The results of the measurements of the diameter of the normal shock wave show that in the case of large flow densities and $M_a < M_{al}$, the diameter of the normal shock wave is a function of

$$D_o/d_a = F\sqrt{n} \tag{2.3}$$

The proportionality factor F in the range of Mach numbers in the nozzle section $1.1 \leq M_a \leq 2.8$ has little dependence on M_a, and can be taken as equal to 0.5 when $n > 20$ for approximate computations. The values of the factor F are shown in Figure 3b, where points 1, ..., 10 correspond to the following combination of parameters (m_a, K_*); 1(1.15, 2.14, 10^{-4}), 2(1.15, 3 x 10^{-4}), /113
3(1.15, f x 10^{-4}), 4(2.27, 1.16 x 10^{-4}), 5(2.27, 1.62 x 10^{-4}), 6(2.27, 10^{-4}), 7(2.27, 5.4 x 10^{-4}), 8(2.8, 1.16 x 10^{-4}), 9(2.8, 1.62 x 10^{-4}), 1.(2.8, 2.7 x 10^{-4}). The results of the investigation of the diameter of the normal shock wave (curves 11 and 12 in Fig. 3b), obtained by the schlieren method and published in [1] and [2], are in good agreement with the data obtained by the visualization of the jet in a glow-discharge for small values of $K_*\sqrt{n}$.

Table 2

M_a	D/x_0	D_0/x_0	C
1.15	0.60	0.54	$2.8\cdot10^{-3}$—$7\cdot10^{-3}$
2.27	0.53	0.41	$1.2\cdot10^{-3}$—$1.7\cdot10^{-3}$
2.5	0.46	0.27	$1.4\cdot10^{-3}$—$1.7\cdot10^{-3}$
2.8	0.39	0.22	$1.1\cdot10^{-3}$—$2.0\cdot10^{-3}$
3.3	0.28		10^{-4}—$2.3\cdot10^{-3}$

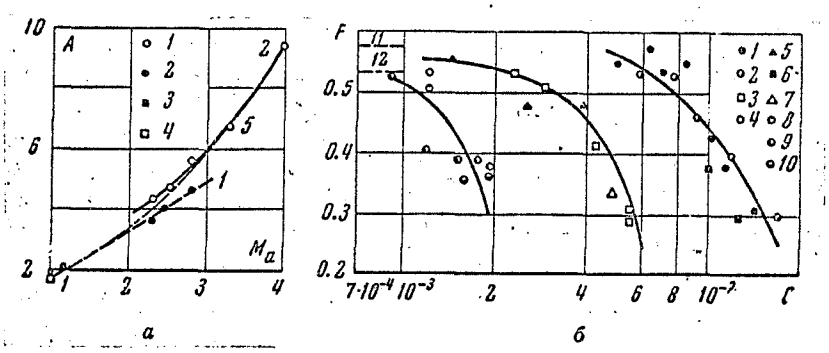

Figure 3. (a) The proportionality factors A and A_1 (2.1) in terms of the Mach number in the nozzle section; (b) f values for different M_a and $K_*\sqrt{n}$.

An increase in the Mach number, M_a, in the nozzle section above some limit, $M_{a1} = f(K_*, n)$ causes a transition from an irregualr reflection of the pendulous shock wave to a regular one (Fig. 2d). At the same time, the angle of incidence of the pendulous shock wave ω (Fig. 4a) drops below the limit $\omega_1 = \arcsin 1/\gamma$ [12].

Figure 4 shows the experimental data for the magnitude of the angle of incidence to the axis of the jet corresponding to the values $M_1 > 10$ and $K_*\sqrt{n} \approx 10^{-3}$. The transition from one type of reflection to the other in the case of large flow densities takes place in what is practically a discontinuity and is accompanied by abrupt reduction in the diameter of the

normal shock wave and in the removal of the point of intersection of the closing discontinuity and the axis of the jet from the nozzle section. The position of the x-discontinuity when $M_a > M_{a1}$ is established by a dependency that is analogous to that at (2.1), but with a different proportionality factor (curve 2 and point 1 in Fig. 3a)

$$A_1 = \sqrt{\gamma} M_a^{3/2} \tag{2.4}$$

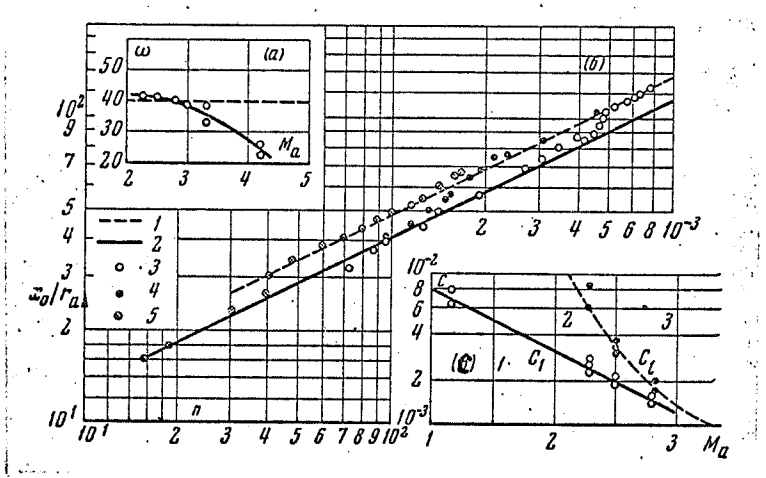

Figure 4. (a) dependence of the angle of incidence of the pendulous shock wave to the jet axis on the Mach number in the nozzle section, M_a; (b) transition of the normal shock wave to the x-discontinuity when M_a = 2.5 and for different K_* with increase in the pressure ratio, n; (c) region of existence of different types of configurations of shock waves near the jet axis; 1 - region of existence of normal shock wave; 2 - region of transition of normal shock wave to the x-discontinuity; 3 - region of existence of x-discontinuity.

The results of the computation for A (curve f, Fig. 3a) using the approximate theory [13] agree satisfactorily with the data from the experiment when $M_a \gg M_{a1}$ and $M_a \ll M_{a1}$ and for high flow densities.

This correspondence does not hold in the transition region.

A change is observed in the geometric characteristics of the curved and of the normal shock waves, expressed first of all by a reduction in the diameter of the normal shock wave in Figure 2, a and b, the result of the increase in the rarefaction of the jet when $M_a < M_{a1}$, because of the reduction in the pressure in the adiabatically slowed down flow, or as a result of the sharp expansion in the case of large pressure ratios, n. In the case of fixed K_* values the onset of the deviation of the D_o/d_a ratio from the value that is typical for the perfect gas flow depends on M_a and on n. The higher the Mach number, for identical K_* values, the sooner the deviation of D_o/d_o from the values established through the dependency at (2.3) will begin.

The parameter C [13] was used to generalize the results obtained with respect to the effect rarefaction has on the flow in the normal shock wave region.

The resluts of the measurements made of the dimensionless diameter of the normal shock wave are shown in Figure 3b, where M_a plays the role of the parameter. With increase in the rarefaction when $c > c_1 = f(M_a, \gamma)$, there is a reduction in the diameter of the normal shock wave, but what also takes place at the same time is the gradual removal of the normal shock wave from the nozzle section. Figure 4b shows the position of the normal shock wave as a function of n when $M_a = 2.5$, and for three values of K_*: $3(1.62 \times 10^{-4})$, $4(2.7 \times 10^{-4})$, $5(5.4 \times 10^{-4})$. Thus, an increase in $C > C_1$ results in the transition of the normal shock wave, the position of which is established by the dependencies at (2.1) and (2.2) (curve 2, Fig. 4b), to the x-discontinuity (Fig. 2b, c), the position of which is established by the dependencies at (2.1) and (2.4) (curve 1, Fig. 4b). /114

The region of the transition of the normal shock wave to the x-discontinuity is shown in Figure 4c in M_a and C coordinates. The transition region is constructed with increase in M_a, and when $M_a \approx 3.3$, and higher, under the conditions of the experiment, there is a regular reflection of the pendulous shock wave from the axis of the jet in Figure 2d. Convexity

of the normal shock wave opposite to the flow (inversion), as in Figure 2b, will be the typical configuration of the normal shock wave in the transition region. This is an irregular supersonic reflection of the shock, along with the formation of a normal shock at number $1.2 \leq M_a < 3.3$ and values for $C < C_l$. When $2.25 \leq M_a < 3.3$ and $C \approx C_l$ the normal shock wave degenerates into the x-discontinuity. The reduction in the normal shock wave when $C > C_1$, and its degeneration into an x-discontinuity when $C \approx C_l$ and a fixed angle of incidence of the diagonal shock wave to the axis of the jet, the value of which is close to the limit (Fig. 4a), can be explained by the reduction in the intensity of the incident shock wave caused by the effect of the dissipative processes.

The results cited show that the Mach number in the nozzle section, determined by the configuration of the pendulous shock wave, as well as the rarefaction of the flow, have an effect on the formation of the flow in the normal shock wave region. An increase in the rarefaction when $C > C_l$ will result in the bulging and blurring of curved shock waves, in a reduction of the intensity of the incident shock wave as compared with the ideal values. The dependence of C_1 and C_l on M_a for $\gamma = 1.4$ is shown in Figure 4c.

Submitted 15 June 1967

REFERENCES

1. Crist, S., Shermann, P. M., Glass, R. D., "Study of the highly underexpanded sonic jet, " AIAA Journal, 1966, Vol. 4, No. 1.

2. Love, E. S., Grigsby, C. E., Lee, L. P., Woodling, M. I., Experimental and theoretical studies of axisymmetric free jets. NASA, TRR-6, 1959.

3. Bier, K. , Schmidt, B., "On the form of shock waves in a freely-expanding gas buoy, " Z. Angew. Phys., 1961, Vol. 13, No. 11.

4. Lewic, C. H., Jr., Carlson, D. J., "Normal shock location in underexpanded gas and gas-particle jets," AIAA Journal, 1964, Vol. 2, No. 4.

5. Yushchenkova, N. I., Nemchenko, V. I., Lyzhnikova, S. A., Vliyaniye kinetiki elementarnykh protsessov na ionizatsiyu sverkhzvukovykh struy nizkotemperaturnoy plazmy. [The effect of kinetics of elementary processes on ionization of hypersonic jets in low-temperature plasma], "Mir" Press, Moscow, 1967.

6. Ginzburg, I. P., Aérogazodinamika. [Aérodynamics], "Vysshaya shkola," Moscow, 1966.

7. Volkonskaya, T. G., "Calculation of hypersonic axisymmetric jets," Sb.: Chislennyye metody v gazovoy dinamike. [Coll.: Calculation methods of gas dynamics], Iz-vo MGU, Moscow, 1963.

8. Kosterin, S. I., Yushchenkova, N. I., Belova, N. T., Kamayer, B. D., "Study of the effect of rarefaction of hypersonic flow on readings of the full thrust probes," Inzh.-fiz. zh., 1962, Vol. 5, No. 12.

9. Daum, F. L., "Air condensation in a hypersonic wind tunnel," AIAA Journal, 1963, Vol. 1, No. 5.

10. McCroskey, W. J., McDougall, J. G., "Shock wave shapes on a sharp flat plate in rarefied hypersonic flow," AIAA Journal, 1966, Vol. 4, No. 1.

11. Korovin, V. M. "On possible simplifications of equations of the dual-temperature partly ionized plasma," PMTF, 1965, No. 6.

12. Osnovy gazovoy dinamiki. [Fundamentals of gas dynamics], "Foreign Literature" Press, Moscow, 1963.

13. Yushchenkova, N. I., Kamayev, B. D., Lyzhnikova, S. A., Nemchenko, V. I. "Structure and parameters of hypersonic jet in low-temperature plasma and transport phenomena in jets," Sb.: Teplofizicheskiye svoystva zhidkostey i gazov pri vysokikh temperaturakh i plazmy.

[Coll.: Thermophysical properties of liquids and gases at high temperature and of the plasma], "Committee for Standards, Measures, and Measuring Instruments" Press, Moscow, 1969.

Translated for the National Aeronautics and Space Administration under contract No. NASw-2038 by Translation Consultants, Ltd., 944 South Wakefield Street, Arlington, Virginia 22204.